Vol. 25, No. 3(2026) Sim26858

Revista Mexicana de Ingeniería Química

Numerical simulation of filtration of a suspension through a radial filter with given flow rate

Simulación numérica de la filtración de una suspensión a través de un filtro radial con caudal de flujo dado

R. Bürger[1]*, B. Kh. Khuzhayorov[2,3], U. Saydullaev[4] and I. Beknazarova[5]

[1]CI^{2}MA and Departamento de Ingeniería Matemática, Facultad de Ciencias Físicas y Matemáticas, Universidad de Concepción, Casilla 160-C, Concepción, Chile

[2]Department of Applied Mathematics, Samarkand State University, 15 University Street, Samarkand City, 140100, Republic of Uzbekistan

[3]V. I. Romanoskiy Institute of Mathematics, Academy of Sciences of Uzbekistan, 100174 Tashkent, Uzbekistan

[4]Department of Theoretical Physics and Quantum Electronics, Engineering Physics Institute, Samarkand State University, 15, University Street, Samarkand City 140100, Uzbekistan

[5]Faculty of English Language, Samarkand State Institute of Foreign Languages, 93 Bostonsaroy Street, Samarkand City 140100, Uzbekistan

Sent: April 28, 2026; Accepted: August 31, 2026

Abstract

The process of filtration of a suspension through a cylindrical filter with a constant flow rate is considered. The suspension is fed through the outer surface of the filter, where a layer of suspended solid particles retained by the filter, called a cake layer, is formed. Given the symmetry, the suspension flow is assumed to be one-dimensional and radial. Suspension filtration equations are derived for the specified conditions. A filtration problem for this equation is posed under the condition of constant suspension flow rate. The problem is solved numerically, and the pressure field distribution for the liquid and solid phases, as well as the cake layer permeability, are determined. The dynamics of cake layer thickness change are also determined. The influence of the parameters relating the concentration of solid particles and permeability to pressure in the solid phase on the filtration characteristics is assessed. These characteristics are the compressive pressure distribution, the cake layer thickness, the solid volume fraction profile, and the relative permeability within the cake layer.

Keywords: Filtration, cake layer, flow rate, numerical simulation.

Resumen

Se considera el proceso de filtración de una suspensión a través de un filtro cilíndrico con un caudal constante. La suspensión se alimenta a través de la superficie exterior del filtro, donde se forma una capa de partículas sólidas retenidas por el filtro, llamada capa de torta. Dada la simetría, se asume que el flujo de la suspensión es unidimensional y radial. Se derivan las ecuaciones de filtración de la suspensión para las condiciones especificadas. Se plantea un problema de filtración para esta ecuación bajo la condición de un caudal constante de suspensión. El problema se resuelve numéricamente y se determinan la distribución del campo de presión para las fases líquida y sólida, así como la permeabilidad de la capa de torta. También se determina la dinámica del cambio en el espesor de la capa de torta. Se evalúa la influencia de los parámetros que relacionan la concentración de partículas sólidas y la permeabilidad con la presión en la fase sólida sobre las características de filtración. Estas características son la distribución del de la presión compresiva, el espesor de la capa de torta, el perfil de la fracción volumétrica de sólidos, y la permeabilidad relativa dentro de la capa de torta.

Palabras clave: Filtración, capa de torta, caudal, simulación numérica

*Corresponding author. E-mail: rburger@ing-mat.udec.cl;
https://doi.org/10.24275/rmiq/Sim26858
ISSN:1665-2738, *issn-e*: 2395-8472

1 Introduction

Filtration of suspension plays an important role in the solid-liquid separation of finely divided solid particles suspended in a viscous fluid. This unit operation is widely used in the chemical, oil and gas, and mining industries (Concha A. and Bascur, 2024; Sparks and Chase, 2015; Tien, 2006; Tien and Ramarao, 2007; Zhuzhikov, 1980) as well as in waste treatment (Bastida-Vázquez et al., 2024; Escobar et al., 2024). Filtration is a hydrodynamic process of separating suspensions into solid and liquid phases using a filter membrane, i.e., a filter. In this process, suspension particles are either retained on the filter surface, where they form a precipitate called a cake layer, or penetrate the filter and become trapped in the pores. Accordingly, two types of filtration are distinguished: cake layer filtration and pore plugging filtration. In cake layer filtration of suspensions, the layer thickness increases in time (Iritani et al., 2018; Shirato et al., 1986; Tien, 2012; Wakeman and Tarleton, 1999).

The basic equations of filtration were among the first to be obtained by Almy and Lewis (1912). In (Zhuzhikov, 1980) and (King, 1980; Tien, 2012) the regularities of filtration processes with the formation of a sediment on the surface of the filter partition are considered. References to models of filtration that include the formation of a cake, as described by traditional filtration theory, include (Bürger et al., 2001; Bürger et al., 2003; Garrido et al., 2003; Khuzhayorov et al., 2023; Tien, 2006; Tien and Bai, 2003; Tien and Ramarao, 2007; Tiller, 1953; Vorobiev, 2022; Wakeman, 1978; Zhuzhikov, 1980). In (2022a, b) a theory is developed where, along with the elasticity of the cake layer, a theory is developed in which, along with the elasticity of the cake layer, irreversible deformation phenomena are incorporated within an explicit elasto-plastic constitutive framework distinguishing loading, unloading, and reloading regimes for axisymmetric cake filtration — extending earlier viscoelastic consolidation models such as the Terzaghi–Voigt approach of Shirato et al. (1986). New equations are derived for loading modes, i.e. in the first stage of filtration, unloading, which occurs after removing the load, and repeated loading. The influence of the plastic properties of the cake layer on the filtration characteristics, including the growth of its thickness, is estimated. Smiles (1970) derives a filtration equation taking into account diffusion. In (Atsumi and Akiyama, 1975), the problem of filtration with cake layer formation was formulated as a problem for a second-order differential equation with a moving boundary, using the Lagrangian approach, and the equation was solved numerically. Using the Eulerian and Lagrangian approaches, a study of filtration with cake layer formation was carried out by Tosun (1986).

Engineering calculations in filtration technology are based on one of two assumptions: either filtration at a constant pressure difference or filtration at a constant flow rate. In the case of filtration at a constant pressure difference, the filtration rate decreases as the cake thickness increases. During filtration at a constant flow rate, an increase in cake thickness leads to an increase in the pressure difference (Zhuzhikov, 1980).

The advantages and disadvantages of filtering mixtures at constant pressure and constant speed were discussed first by Tiller (1953) and then in (Greil et al., 1992; Mahdi and Holdich, 2013, 2017; Mahdi et al., 2019). Studies comparing the results of filtering mixtures at constant pressure and constant speed were conducted Tarabara et al. (2002) and Yim et al. (2003).

Furthermore, we mention that Kalantariasl and Bedrikovetsky (2014) studied the stabilization of an external filter cake by colloidal forces in a well–reservoir system, derived the mechanical equilibrium equation governing cake stabilization, and proposed an analytical model describing the conditions under which the external cake reaches a stable configuration. On the other hand, Kalantariasl et al. (2014) developed an analytical model for axi-symmetric two-phase suspension–colloidal flow in porous media during water injection, in which deep-bed filtration of particles, formation of an external filter cake, and cake stabilization due to particle mobilization are accounted for simultaneously; explicit formulae for the pressure drop (impedance) across the system were derived under the assumption of an incompressible cake. Finally, Kalantariasl et al. (2015) proposed a mathematical model for the non-uniform external filter cake profile that develops along long injection wells. The present work can be compared with the cited works by Kalantariasl at al., as will be discussed in Section 5.

It is the purpose of the present work to examine the filtration of suspensions through a cylindrical filter with a constant flow rate, that is, we focus on constant rate filtration (CRF), as opposed to constant-pressure filtration (CPF). In fact, recent literature (Iritani, 2003; Mahdi and Holdich, 2013; Mahdi et al., 2019) highlights why focusing on CRF is essential for the reliability of our study as compared to constant pressure filtration (CPF): CRF allows for a more accurate determination of the filter medium resistance R_{m}, while time versus filtrate rate plots within CPF often yield unreliable filter medium resistance values (in fact, CRF provides stable data from the very start, allowing for more accurate determination of stabilized resistance; moreover, CRF allows us to monitor the initial resistance increase caused by “clogging” or “blinding” more effectively; and CRF promotes a more uniform packing structure independent of cake thickness, providing a more stable

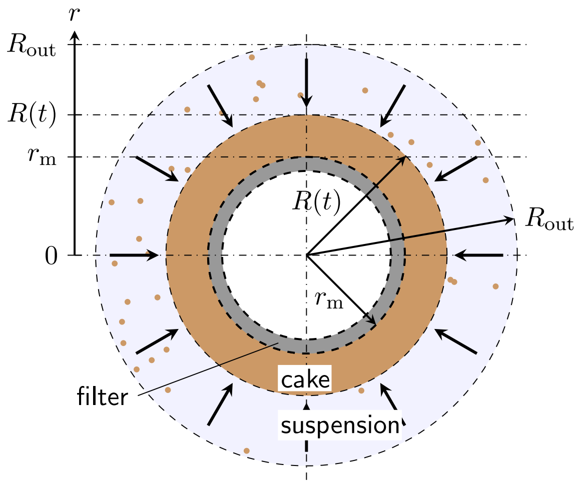

Fig. 1. Schematic of a suspension filtering through a cylindrical filter.

basis for mathematical modeling, see Section *2.5*.

The specific setup of CRF is as follows. The suspension is fed through the outer surface of the filter cell, which is supposed to have a fixed radius R_{out}. As it passes through the filter, suspension particles are retained. These particles form a cylindrical cake layer on the filter surface. It is assumed that filtration occurs in the radial direction, i.e., the direction of movement of the liquid and suspended particles coincides with the radial direction. Consequently, the flow can be considered one-dimensional and radially axisymmetric. In this work, the assumption of one-dimensional radial flow is based on the cylindrical symmetry of the filter geometry, which applies to a number of industrially relevant devices that do not require rotation to operate. In the oil and gas industry, cylindrical filter elements are installed around injection wells in the wellbore region. In water injection operations, particle-laden fluid is forced radially through the screen into the formation, accumulating a cake layer on the screen surface under essentially constant injection velocity conditions. This represents the precise scenario modeled by our study (Kalantariasl et al., 2014, 2015). On the other hand, in the chemical and polymer industries, the suspension surrounds a cylindrical candle element; the cake accumulates on the outer surface, and the filtrate is collected from the interior core. When connected to a positive displacement pump, these devices operate at a constant flow rate, making the CRF framework of this study directly applicable (Sparks and Chase, 2015).

Filtration equations are developed taking these conditions into account. These equations are then solved numerically, determining the pressure fields for the liquid and solid phases, the change in solid phase content, and the relative permeability in the cake layer. The growth of the cake layer thickness over time is also determined. The influence of the compressibility exponent β and the permeability exponent δ, which relate the solid volume fraction and the cake permeability to the compressive pressure through power-law constitutive relations (see Eq. (11) in Section *2.2*), is assessed on the compressive pressure distribution $p_{\text{s}}(t,r)$, the cake layer thickness $R(t)-r_{\text{m}}$, the solid volume fraction profile $\varepsilon_{\text{s}}(t,r)$, and the relative permeability k/k^0 within the cake layer.

2 Model formulation

2.1 Assumptions of the model

In this work, a cylindrical filter of radius r_{m} and height h is considered (see Figure 1); since the suspension flow is one-dimensional, that is, purely radial, all field variables — the solid volume fraction ε_{s}, the compressive pressure p_{s}, and the liquid pressure p_ℓ — are functions of t and t only. Filtration is carried out under constant flow rate conditions. The local structure of the cake layer — in particular, the solid volume fraction ε_{s} and the permeability k — is assumed to depend on p_{s} through power-law relations (see Eq. (11) in Section *2.2*), which have been validated experimentally in the literature (Tiller and Leu, 1980; Stamatakis and Tien, 1991). These assumptions complement those adopted in the earlier works of the principal author (Khuzhayorov et al., 2022a, 2022b, 2023), in which filtration through a planar filter under constant pressure conditions or with the formation of an elasto-plastic cake was studied.

2.2 Filtration equations with cake formation

The filter material is a cylindrical surface with radius r_{m} and height h. The cake layer grows in the outer part $r \geq r_{\text{m}}$, and the cake-suspension interface is denoted by $R(t)$. The cake occupies a region $r_{\text{m}} \leq r \leq R(t)$ with $R(t) \geq r_{\text{m}}$ and $\mathrm{d}R/\mathrm{d}t \geq 0$, where t is time. The liquid flows in the direction of decreasing r. In what follows, we assume that all field variables are independent of height and azimuthal angle, so that they depend on r and t only. If $\varepsilon_{\text{s}} = \varepsilon_{\text{s}}(t,r)$ is the relative content of solid phases (solid volume fraction), $q_\ell = q_\ell(t,r)$ is the filtration rate of the liquid phase, and $q_{\text{s}} = q_{\text{s}}(t,r)$ is the filtration rate of the solid phase, then q_ℓ and q_{s} are negative in the direction r. If we recall that if $v_\ell = v_\ell(t,r)$ and $v_{\text{s}} = v_{\text{s}}(t,r)$ are the liquid and solid phase velocities, then this means that

$$q_\ell = -(1-\varepsilon_{\text{s}})v_\ell \quad \text{and} \quad q_{\text{s}} = -\varepsilon_{\text{s}} v_{\text{s}}. \qquad (1)$$

The suspension is located outside the cake layer at $r > R(t)$. The fundamental equations describing cake formation include the continuity equations, the Darcy equation (Shirato et al., 1969; Tien, 2006; Tien and Ramarao, 2007), the momentum balance equation, and equations relating cake structure (solid phase density, permeability, or resistivity) to the compressive stress experienced by the solid particles. The continuity equations for the solid and liquid phases of the suspension are

$$\begin{aligned} \frac{\partial \varepsilon_{\mathrm{s}}}{\partial t} + \frac{1}{r}\frac{\partial}{\partial r}(r q_{\mathrm{s}}) = 0 \quad \text{and} \\ \frac{\partial (1-\varepsilon_{\mathrm{s}})}{\partial t} + \frac{1}{r}\frac{\partial}{\partial r}(r q_{\ell}) = 0, \end{aligned} \tag{2}$$

from which we infer that

$$\frac{1}{r}\frac{\partial}{\partial r}(r(q_{\mathrm{s}} + q_{\ell})) = 0, \tag{3}$$

which implies that $r(q_{\mathrm{s}} + q_{\ell})$ is a function $\mathcal{F} = \mathcal{F}(t)$ of time only, i.e., $r(q_{\mathrm{s}} + q_{\ell}) = \mathcal{F}(t)$. Thus, defining $q_{\ell \mathrm{m}} \coloneqq q_{\mathrm{s}} + q_{\ell}$, we assume that

$$r(q_{\mathrm{s}} + q_{\ell}) = r q_{\ell \mathrm{m}} = \mathcal{F}(t). \tag{4}$$

On the other hand, Darcy's law in a multi-dimensional setting is usually written as

$$\boldsymbol{q} = -\frac{k}{\mu}\nabla p_{\ell}, \tag{5}$$

where $\boldsymbol{q}$ is the "Darcy velocity" or "Darcy flux," p_{ℓ} is the pressure in the liquid phase, k is the permeability, and μ is the viscosity of the suspension. Notice that $\boldsymbol{q}$ is not the velocity at which the fluid is travelling through the pores; rather, it is the volumetric flux, or flow rate per unit area (see Stauffer, 2006). The actual pore velocity, that is the fluid-solid relative velocity $\boldsymbol{v}_{\ell} - \boldsymbol{v}_{\mathrm{s}}$, where $\boldsymbol{v}_{\ell}$ and $\boldsymbol{v}_{\mathrm{s}}$ are the fluid and solid phase velocities, is related to $\boldsymbol{q}$ by

$$\boldsymbol{v}_{\ell} - \boldsymbol{v}_{\mathrm{s}} = \frac{1}{1-\varepsilon_{\mathrm{s}}}\boldsymbol{q}, \tag{6}$$

where we recall that $1 - \varepsilon_{\mathrm{s}}$ is the local porosity. Under the conditions of one-dimensional horizontal radial flow, as in many petroleum and hydrogeological applications (like flow toward a well), we may assume that $k = k(t,r)$, $p_{\ell} = p_{\ell}(t,r)$, $\boldsymbol{q} = q = q(t,r)$, $\boldsymbol{v}_{\ell} = v_{\ell}(t,r)$ and $\boldsymbol{v}_{\mathrm{s}} = v_{\mathrm{s}}(t,r)$ and Darcy's law (5) takes the form

$$q = -\frac{k}{\mu}\frac{\partial p_{\ell}}{\partial r}. \tag{7}$$

Combining (6) and (7) we get

$$v_{\ell}(t,r) - v_{\mathrm{s}}(t,r) = -\frac{k}{(1-\varepsilon_{\mathrm{s}})\mu}\frac{\partial p_{\ell}}{\partial r}. \tag{8}$$

Finally, we employ (1) to obtain the filtration law

$$\frac{q_{\ell}}{1-\varepsilon_{\mathrm{s}}} - \frac{q_{\mathrm{s}}}{\varepsilon_{\mathrm{s}}} = \frac{1}{1-\varepsilon_{\mathrm{s}}}\frac{k}{\mu}\frac{\partial p_{\ell}}{\partial r}, \tag{9}$$

where we recall that $p_{\ell} = p_{\ell}(t,r)$ is the pressure in the liquid phase, $k = k(t,r)$ is the permeability, and μ is the viscosity of the suspension. Equation (9) represents a generalized form of Darcy's law for the region where the cake layer is forming. The parameter $k(t,r)$ is the permeability coefficient of the filter cake generated during the filtration process, which varies over time and space as a result of particle compaction.

In the equations for conservation of momentum for the phases, inertial effects and the action of mass forces on the phases are neglected. Then, by summing the equations for the phases and taking into account that the interaction forces are mutually opposite, one obtains a zero sum of the forces acting on the phases. Ignoring the forces of viscous friction, this reasoning relationship (see Tien (2012))

$$\mathrm{d}p_{\ell} + \mathrm{d}p_{\mathrm{s}} = 0, \tag{10}$$

where p_{s} is the compressive pressure, and which implies that $\partial p_{\ell}/\partial p_{\mathrm{s}} = -1$. This relation is consistent with the classical assumption first proposed on intuitive physical grounds by Ruth (1935) and Tiller (1953), and forms the basis of most traditional cake filtration theory (Tien, 2006; Tien and Ramarao, 2007). Equation (10) follows from summing the phase momentum balances after neglecting (i) inertial effects, (ii) body forces, and, critically, (iii) the viscous shear stresses within each phase — only the interphase drag (interaction) force and the phase pressure gradients are retained, and since the drag forces on the two phases are equal and opposite, they cancel upon summation, leaving (10). This simplification is expected to be reasonable when the filtration (Darcy) velocity is small, so that viscous shear within each phase is negligible compared to the interphase drag and to the pressure gradients themselves — that is, in the same low-Reynolds-number, slow seepage-flow regime in which Darcy's law itself is valid (typically $\mathrm{Re} \ll 1$ based on the pore-scale velocity and particle size). That said, similar but different expressions that involve coefficients depending on the solids volume fraction ε_{s}, also called "solidosity," and the corresponding liquid volume fraction $1 - \varepsilon_{\mathrm{s}}$ may be derived by multiphase flow theory and carrying out volume averaging of the continuity equations (momentum) of the particulate and liquid phases. These alternative expressions (not used herein) and their consequences are compared by Tien et al. (2001).

In the filter cake, the solids volume fraction ε_{s} and the permeability k are assumed be functions of the compressive pressure p_{s} of the form (see Stamatakis and Tien (1991); Tien (2012); Tiller and Leu (1980))

$$\varepsilon_{\mathrm{s}} = \varepsilon_{\mathrm{s}}^{0}(1 + p_{\mathrm{s}}/p_A)^{\beta}, \quad k = k^{0}(1 + p_{\mathrm{s}}/p_A)^{\delta}, \tag{11}$$

where $\varepsilon_{\mathrm{s}}^{0}$ and k^{0} are the values of ε_{s} and k, respectively, at zero compressive pressure ($p_{\mathrm{s}} = 0$), p_A is a material specific (characteristic) parameter, and β and δ are material specific, constant exponents.

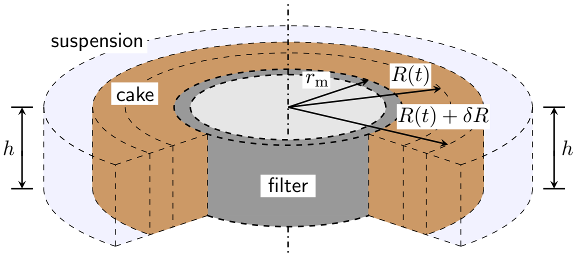

Fig. 2. Derivation of the condition at the moving boundary $R(t)$.

The Darcy equation (9) can be rewritten as

$$q_\ell - \frac{1-\varepsilon_{\mathrm{s}}}{\varepsilon_{\mathrm{s}}} q_{\mathrm{s}} = \frac{k}{\mu}\frac{\partial p_\ell}{\partial r}. \tag{12}$$

From (4) and (12) we obtain

$$q_\ell = \varepsilon_{\mathrm{s}} \frac{k}{\mu}\frac{\partial p_\ell}{\partial r} + (1-\varepsilon_{\mathrm{s}}) q_{\ell \mathrm{m}}. \tag{13}$$

Substituting (13) into the first equation of (2) we obtain

$$\begin{aligned} \frac{\partial \varepsilon_{\mathrm{s}}}{\partial t} &= -\frac{1}{r}\frac{\partial}{\partial r}\left(r\left(\varepsilon_{\mathrm{s}} \frac{k}{\mu}\frac{\partial p_\ell}{\partial r} + (1-\varepsilon_{\mathrm{s}}) q_{\ell \mathrm{m}}\right)\right) \\ &= -\frac{1}{r}\frac{\partial}{\partial r}\left(r\varepsilon_{\mathrm{s}} \frac{k}{\mu}\frac{\partial p_\ell}{\partial r}\right) - \frac{1}{r}\left(\frac{\partial}{\partial r}(1-\varepsilon_{\mathrm{s}})\right) r q_{\ell \mathrm{m}} \\ &\quad - \frac{1}{r}(1-\varepsilon_{\mathrm{s}})\frac{\partial}{\partial r}(r q_{\ell \mathrm{m}}). \end{aligned} \tag{14}$$

Since $rq_{\ell \mathrm{m}}$ does not depend on r, the third term in the last right-hand side is zero. Thus, recalling that $rq_{\ell \mathrm{m}} = \mathcal{F}(t)$, we get

$$\frac{\partial \varepsilon_{\mathrm{s}}}{\partial t} = -\frac{1}{r}\frac{\partial}{\partial r}\left(r\varepsilon_{\mathrm{s}} \frac{k}{\mu}\frac{\partial p_\ell}{\partial r}\right) + \frac{\mathcal{F}(t)}{r}\frac{\partial \varepsilon_{\mathrm{s}}}{\partial r}. \tag{15}$$

We wish to solve (15) for $p_{\mathrm{s}} = p_{\mathrm{s}}(t,r)$ as the governing unknown, which requires a suitable boundary condition at the moving boundary $r = R(t)$.

2.3 *Condition at the moving boundary $R(t)$*

We now define the equation for a moving boundary $R(t)$, which characterizes the growth of a sediment layer (cake layer). We consider a thin annular control volume consisting of a cylindrical shell located at the cake-suspension interface $r = R(t)$, of radial thickness $\delta R \geq 0$ and height h, so that its lateral surface area is $2\pi R(t)h$ (see Figure 2). Over a short time interval δt, the boundary $R(t)$ moves outward by δR, and the shell — which was occupied by suspension at time t — becomes part of the cake at time $t+\delta t$. The integral mass balance for the liquid phase within this control volume over the time interval δt takes the standard form

$$V_{\mathrm{in}} - V_{\mathrm{out}} = V_{\mathrm{acc}}, \tag{16}$$

where the three terms are evaluated explicitly as follows. The inlet flux (from the cake side, $r = R(t)^-$): the liquid filtration rate at the inner surface of the control volume is $q_{\ell \mathrm{i}}$, acting over the surface area $2\pi R(t)h$ during the time interval δt, giving

$$V_{\mathrm{in}} = q_{\ell \mathrm{i}} \cdot 2\pi R(t) h \delta t; \tag{17}$$

the outlet flux (from the suspension side, $r = R(t)^+$): the liquid filtration rate at the outer surface is $q_{\ell \mathrm{o}}$, giving

$$V_{\mathrm{out}} = q_{\ell \mathrm{o}} \cdot 2\pi R(t) h \delta t; \tag{18}$$

the accumulation (rate of change of liquid volume within the control volume): at time t, the shell of thickness δR is filled with suspension having liquid volume fraction $1-\varepsilon_{\mathrm{s}0}$, and therefore contains a liquid volume of $(1-\varepsilon_{\mathrm{s}0})2\pi R(t)h\delta R$. At time $t+\delta t$, the same shell has become part of the cake with liquid volume fraction $1-\varepsilon_{\mathrm{s}}^0$, since the compressive pressure vanishes at the freshly formed cake surface, $p_{\mathrm{s}} = 0$ at $r = R(t)$, so that $\varepsilon_{\mathrm{s}} = \varepsilon_{\mathrm{s}}^0$ follows from Eq. (11), and therefore the shell contains a liquid volume of $(1-\varepsilon_{\mathrm{s}}^0)2\pi R(t)h\delta R$. Consequently, the net change of liquid volume within the control volume over the time interval δt is

$$\begin{aligned} V_{\mathrm{acc}} &= ((1-\varepsilon_{\mathrm{s}}^0) - (1-\varepsilon_{\mathrm{s}0}))2\pi R(t)h\delta R \\ &= (\varepsilon_{\mathrm{s}0} - \varepsilon_{\mathrm{s}}^0)2\pi R(t)h\delta R. \end{aligned} \tag{19}$$

Substituting all three terms into (16) and dividing both sides by $2\pi Rh\delta t$, we arrive at

$$\begin{aligned} (q_{\ell \mathrm{i}} - q_{\ell \mathrm{o}})\delta t &= ((1-\varepsilon_{\mathrm{s}}^0) - (1-\varepsilon_{\mathrm{s}0}))\delta R \\ &= (\varepsilon_{\mathrm{s}0} - \varepsilon_{\mathrm{s}}^0)\delta R, \end{aligned} \tag{20}$$

and taking $\delta t \to 0$ we obtain

$$\frac{\mathrm{d}R}{\mathrm{d}t} = \frac{q_{\ell \mathrm{i}} - q_{\ell \mathrm{o}}}{\varepsilon_{\mathrm{s}0} - \varepsilon_{\mathrm{s}}^0} \tag{21}$$

and similarly, for the solid phase,

$$\frac{\mathrm{d}R}{\mathrm{d}t} = \frac{q_{\mathrm{si}} - q_{\mathrm{so}}}{\varepsilon_{\mathrm{s}0} - \varepsilon_{\mathrm{s}}^0}. \tag{22}$$

To determine expressions for $q_{\ell \mathrm{i}}$ and $q_{\ell \mathrm{o}}$, we use physical laws and assumptions and examine the situation in the vicinity of $R(t)$, where by $r = R(t)^-$ and $r = R(t)^+$ we denote limits for $r \to R(t)$ taken for $r < R(t)$ and $r > R(t)$, respectively. Within the cake, Darcy's law (12) is in effect, hence

$$q_{\ell \mathrm{i}} - \frac{1-\varepsilon_{\mathrm{s}}^0}{\varepsilon_{\mathrm{s}}^0} q_{\mathrm{si}} = \left.\left(\frac{k}{\mu}\frac{\partial p_{\mathrm{s}}}{\partial r}\right)\right|_{r=R(t)^-}. \tag{23}$$

Since on the border $R(t)$, there hold $p_{\mathrm{s}} = 0$, $\varepsilon_{\mathrm{s}} = \varepsilon_{\mathrm{s}}^0$ and also $q_{\ell \mathrm{i}} + q_{\mathrm{si}} = q_{\ell \mathrm{m}}$, that is, $q_{\mathrm{si}} = q_{\ell \mathrm{m}} - q_{\ell \mathrm{i}}$, we obtain from (23)

$$q_{\ell \mathrm{i}} - \frac{1-\varepsilon_{\mathrm{s}}^0}{\varepsilon_{\mathrm{s}}^0}(q_{\ell \mathrm{m}} - q_{\ell \mathrm{i}}) = \left.\left(\frac{k}{\mu}\frac{\partial p_{\mathrm{s}}}{\partial r}\right)\right|_{r=R(t)^-} \tag{24}$$

or equivalently,

$$q_{\ell \mathrm{i}} = \left(\varepsilon_{\mathrm{s}}^{0} \frac{k}{\mu} \frac{\partial p_{\mathrm{s}}}{\partial r} \right) \bigg|_{r=R(t)^-} + (1-\varepsilon_{\mathrm{s}}^{0}) q_{\ell \mathrm{m}}. \tag{25}$$

In the suspension zone, we assume that the liquid and solid phases move at the same velocity, which implies that

$$\frac{q_{\ell \mathrm{o}}}{1-\varepsilon_{\mathrm{s}0}} = \frac{q_{\mathrm{so}}}{\varepsilon_{\mathrm{s}0}} \tag{26}$$

or equivalently,

$$\frac{q_{\ell \mathrm{o}}}{q_{\mathrm{so}}} = \frac{1-\varepsilon_{\mathrm{s}0}}{\varepsilon_{\mathrm{s}0}}. \tag{27}$$

Since $q_{\ell \mathrm{o}} + q_{\mathrm{so}} = q_{\ell \mathrm{m}}$, we obtain $q_{\ell \mathrm{o}} = (1-\varepsilon_{\mathrm{s}0}) q_{\ell \mathrm{m}}$. Now substituting $q_{\ell \mathrm{i}}$ from (25) and $q_{\ell \mathrm{o}}$ into the liquid mass balance (21) yields

$$\begin{aligned} \frac{\mathrm{d}R}{\mathrm{d}t} &= \frac{1}{\varepsilon_{\mathrm{s}0} - \varepsilon_{\mathrm{s}}^{0}} \left(\left(\varepsilon_{\mathrm{s}}^{0} \frac{k}{\mu} \frac{\partial p_{\mathrm{s}}}{\partial r} \right) \bigg|_{r=R(t)^-} \right. \\ &\quad \left. + (1-\varepsilon_{\mathrm{s}}^{0}) q_{\ell \mathrm{m}} - (1-\varepsilon_{\mathrm{s}0}) q_{\ell \mathrm{m}} \right) \\ &= -\frac{\varepsilon_{\mathrm{s}}^{0}}{\varepsilon_{\mathrm{s}}^{0} - \varepsilon_{\mathrm{s}0}} \left(\frac{k}{\mu} \frac{\partial p_{\mathrm{s}}}{\partial r} \right) \bigg|_{r=R(t)^-} + q_{\ell \mathrm{m}}. \end{aligned} \tag{28}$$

Finally, we take into account that $q_{\ell \mathrm{m}}$ is not a constant; rather, there holds $q_{\ell \mathrm{m}} = \mathcal{F}(t)/r$. Since $q_{\ell \mathrm{m}}$ is therefore a continuous function of r (for $r > 0$) and t (under suitable assumptions on $\mathcal{F}$), we get $q_{\ell \mathrm{m}} = \mathcal{F}(t)/R(t)$ for $r = R(t)^-$. Thus, (28) can be written as

$$\frac{\mathrm{d}R}{\mathrm{d}t} = -\frac{\varepsilon_{\mathrm{s}}^{0}}{\varepsilon_{\mathrm{s}}^{0} - \varepsilon_{\mathrm{s}0}} \left(\frac{k}{\mu} \frac{\partial p_{\mathrm{s}}}{\partial r} \right) \bigg|_{r=R(t)^-} + \frac{\mathcal{F}(t)}{R(t)}. \tag{29}$$

In the present work we assume that $\mathcal{F}$ is a constant. The value of $\mathcal{F}$ is determined if $q_{\ell \mathrm{m}}$ is known at a given radial position r. With respect to the setup of Figure 1 it is natural that $q_{\ell \mathrm{m}}$ is specified for $r = R_{\mathrm{out}}$. If we consider constant flow and set $q_{\ell \mathrm{m}}(r,t) = q_{\ell \mathrm{m,in}}$ for $r = R_{\mathrm{out}}$, then we obtain

$$\mathcal{F} = q_{\ell \mathrm{m,in}} R_{\mathrm{out}}. \tag{30}$$

In what follows we assume that (30) is in effect.

2.4 *Initial conditions*

When the filtration process starts with a given initial flow velocity, we can take the initial condition for p_{s} to be equal to zero, i.e.,

$$p_{\mathrm{s}}(0,r) = 0. \tag{31}$$

On the other hand, if the filtration process begins without preliminary pumping of liquid, we can adopt the initial condition $R(0) = r_{\mathrm{m}}$.

2.5 *Boundary conditions for constant-flow operation*

At the cake-suspension border we impose

$$\varepsilon_{\mathrm{s}}(t,R(t)) = \varepsilon_{\mathrm{s}0}, \quad p_{\mathrm{s}}(t,R(t)) = 0 \quad \text{for } t > 0. \tag{32}$$

On the other hand, concerning the boundary condition at $r = r_{\mathrm{m}}$, we comment filter medium resistance fully reflects the physical nature of the CRF process. Indeed, under CRF conditions the filtration rate $\mathcal{F}$ remains constant ($\mathcal{F} = rq_{\ell \mathrm{m}} = \text{const.}$). Therefore, at the very beginning of the process ($t = 0$), when the cake layer has not yet formed, the entire hydraulic resistance is represented solely by R_{m}. As reported by Mahdi and Holdich (2017) and Mahdi et al. (2019), in CRF the intercept of the pressure–time relationship (Δp versus t) with the vertical axis at $t = 0$ is directly equal to $\mu q_{\ell \mathrm{m}} R_{\mathrm{m}}$. This makes it possible to determine R_{m} very accurately from experimental data. As the cake layer grows, the cake resistance increases progressively, while the filter medium resistance remains constant. In fact, physically, R_{m} is a lumped parameter characterizing the hydraulic resistance of the filter medium (the rigid porous septum), as distinct from the cake permeability $k = k(p_{\mathrm{s}})$, which is a property of the deposited and compacting particulate material described by Eq. (11). The two quantities play fundamentally different roles in the model: the cake permeability k evolves in space and time as the cake grows and compacts under the compressive pressure p_{s}, while R_{m} is treated as a constant material property of the rigid, non-deforming filter medium, independent of p_{s}, and of time.

In contrast to CRF, in constant pressure filtration (CPF), the high pressure at the beginning of the process often leads to a "clogging" effect, which makes the estimation of R_{m} unstable. In the CRF model, however, this behavior is controlled through the boundary condition, ensuring a more stable description of the process. Therefore, it is appropriate to write the boundary condition on the filter material in the form

$$\begin{aligned} \frac{\mathcal{F}}{r_{\mathrm{m}}} &= q_{\ell \mathrm{m}} = -\left(\frac{k}{\mu} \frac{\partial p_{\mathrm{s}}}{\partial r} \right) \bigg|_{r=r_{\mathrm{m}}} \\ &= \frac{p_{\ell}}{R_{\mathrm{m}} \mu} = \text{const.} \quad (q_{\ell \mathrm{m}} \geq 0). \end{aligned} \tag{33}$$

For ease of notation we define

$$\eta_{\mathrm{s}} := 1 + p_{\mathrm{s}}/p_A. \tag{34}$$

Then, utilizing (10) and (11), we may convert (15) into a PDE for p_{s}. This yields

$$\begin{aligned} \frac{\varepsilon_{\mathrm{s}}^{0} \beta}{p_A} \eta_{\mathrm{s}}^{\beta-1} \frac{\partial p_{\mathrm{s}}}{\partial t} &= \frac{1}{r} \frac{\partial}{\partial r} \left(r \frac{\varepsilon_{\mathrm{s}}^{0} k^{0}}{\mu} \eta_{\mathrm{s}}^{\beta-\delta} \frac{\partial p_{\mathrm{s}}}{\partial r} \right) \\ &\quad + \frac{\mathcal{F}}{r} \frac{\varepsilon_{\mathrm{s}}^{0} \beta}{p_A} \eta_{\mathrm{s}}^{\beta-1} \frac{\partial p_{\mathrm{s}}}{\partial r} \end{aligned} \tag{35}$$

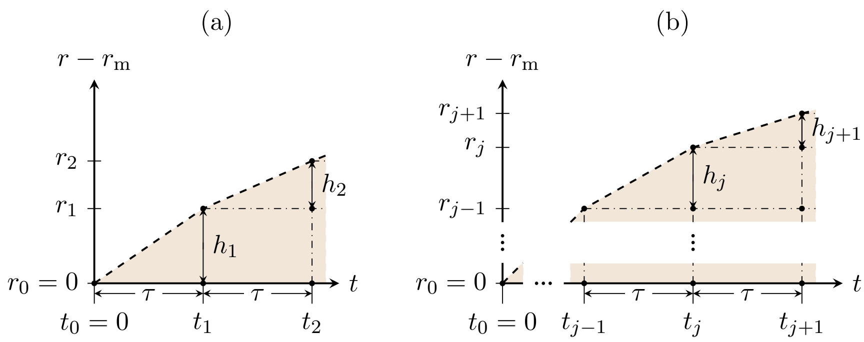

Fig. 3. (a) Initial computational domain, (b) computational domain for the computation of ϕ_i^{j+1}.

or equivalently,

$$\frac{\partial p_{\mathrm{s}}}{\partial t} = \frac{p_A k^0}{\mu\beta}\eta_{\mathrm{s}}^{1-\beta}\frac{1}{r}\frac{\partial}{\partial r}\left(r\eta_{\mathrm{s}}^{\beta-\delta}\frac{\partial p_{\mathrm{s}}}{\partial r}\right) + \frac{\mathcal{F}}{r}\frac{\partial p_{\mathrm{s}}}{\partial r}. \tag{36}$$

On the other hand, equation (29) for the free boundary is reduced to

$$\frac{\mathrm{d}R}{\mathrm{d}t} = -\frac{\varepsilon_{\mathrm{s}}^0}{\varepsilon_{\mathrm{s}}^0 - \varepsilon_{\mathrm{s}0}}\left(\frac{k^0}{\mu}\eta_{\mathrm{s}}^{-\delta}\frac{\partial p_{\mathrm{s}}}{\partial r}\right)\bigg|_{r=R(t)^-} + \frac{\mathcal{F}}{R(t)}. \tag{37}$$

2.6 Free boundary problem in final form

Defining the expressions

$$\begin{aligned} a(p_{\mathrm{s}}) &:= \frac{p_A k^0}{\mu\beta}\eta_{\mathrm{s}}^{1-\beta}, \quad b(p_{\mathrm{s}}) := \eta_{\mathrm{s}}^{\beta-\delta}, \\ d(p_{\mathrm{s}}) &:= \frac{\varepsilon_{\mathrm{s}}^0}{\varepsilon_{\mathrm{s}}^0 - \varepsilon_{\mathrm{s}0}}\frac{k^0}{\mu}\eta_{\mathrm{s}}^{-\delta}, \quad \text{and} \\ g(p_{\mathrm{s}}) &:= \frac{k^0}{\mu}\eta_{\mathrm{s}}^{-\delta}, \end{aligned} \tag{38}$$

and taking into account (30), we may formulate the PDE for $p_{\mathrm{s}} = p_{\mathrm{s}}(t,r)$ (36), the ODE for the evolution of $R = R(t)$ (37), and the boundary condition at the filter material (33) as follows, where $t > 0$:

$$\begin{aligned} \frac{\partial p_{\mathrm{s}}}{\partial t} &= a(p_{\mathrm{s}})\frac{1}{r}\frac{\partial}{\partial r}\left(rb(p_{\mathrm{s}})\frac{\partial p_{\mathrm{s}}}{\partial r}\right) \\ &\quad + \frac{q_{\ell\mathrm{m,in}}R_{\mathrm{out}}}{r}\frac{\partial p_{\mathrm{s}}}{\partial r}, \quad r_{\mathrm{m}} < r < R(t), \end{aligned} \tag{39}$$

$$\frac{\mathrm{d}R}{\mathrm{d}t} = -\left(d(p_{\mathrm{s}})\frac{\partial p_{\mathrm{s}}}{\partial r}\right)\bigg|_{r=R(t)^-} + \frac{q_{\ell\mathrm{m,in}}R_{\mathrm{out}}}{R(t)}, \tag{40}$$

$$\frac{q_{\ell\mathrm{m,in}}R_{\mathrm{out}}}{r_{\mathrm{m}}} = -g(p_{\mathrm{s}})\frac{\partial p_{\mathrm{s}}}{\partial r}\bigg|_{r=r_{\mathrm{m}}} = \text{const.} \tag{41}$$

The solution of the system of equations (39)–(41) together with the corresponding initial condition (31) and boundary conditions (32) and (33) determines the filtration characteristics. We recall that $R(t)$ is not given beforehand; rather, (40) stipulates that the evolution of the boundary $R(t)$ depends on the solution $p_s(t,r)$ in the interior of the computational domain, hence (39)–(41) is a free boundary problem.

3 Numerical method

The free boundary problem (31), (32), (33), (39)–(41) is approximately solved by a finite difference method (Caldwell and Kwan, 2004; Khuzhayorov et al., 2023, 2022a,b; Samarsky and Vabishchevich, 2003). Since the problem under consideration has a free boundary (that is, an unknown moving boundary), we use a version of the finite difference method with frontier detection by coordinate r for a given moment of time t. New nodes of this grid will be determined from the condition that the moving boundary coincides with this node.

3.1 Finite-difference approximation

Assume that τ is a fixed time step and that at time $t = t_{j+1} = (j+1)\tau$ the spatial grid consists of nodes $r_0 = 0$ (corresponding to $r = r_{\mathrm{m}}$) and $r_i = r_{i-1} + h_i$ for $i = 1,\dots,j+1$, where the position of the boundary node r_{j+1}, that is, $h_{j+1} = r_{j+1} - r_j$ (see Figure 3(b)) is unknown. We denote the approximate value of p_{s} at the point (t_j, r_i) by ϕ_i^j. The partial differential equation (39) is approximated by an implicit difference scheme that is nonlinear with respect to ϕ_i^{j+1}. To describe the scheme it is useful to introduce difference operators Δ_- and Δ_+ that act on the spatial index i, i.e., $\Delta_- a_i := a_i - a_{i-1}$ and $\Delta_+ a_i := a_i - a_{i-1}$. Furthermore, we define $r_{i+1/2} := (r_i + r_{i+1})/2$ and

$$\eta_{\mathrm{s}i}^j := 1 + \phi_i^j / p_A. \tag{42}$$

Then we get

$$\begin{aligned} &\frac{\phi_i^{j+1} - \phi_i^j}{\tau} - \frac{2a(\phi_i^{j+1})}{r_i(h_i + h_{i+1})}\times \\ &\times \Delta_-\left(b(\phi_i^{j+1}, \phi_{i+1}^{j+1})r_{i+1/2}\frac{\phi_{i+1}^{j+1} - \phi_i^{j+1}}{h_{i+1}}\right) \\ &+ \frac{q_{\ell\mathrm{m,in}}R_{\mathrm{out}}}{r_{i-1/2}}\frac{\phi_i^{j+1} - \phi_{i-1}^{j+1}}{h_i} = 0, \quad i = 1,\dots,j, \end{aligned} \tag{43}$$

where we define

$$b(\phi_i^{j+1},\phi_{i+1}^{j+1}) := \frac{1}{2}\Big((\eta_{s,i+1}^{j+1})^{\beta-\delta} + (\eta_{s,i}^{j+1})^{\beta-\delta}\Big), \tag{44}$$

$$a(\phi_i^{j+1}) := \frac{p_A k^0}{\mu\beta}(\eta_{s,i}^{j+1})^{1-\beta}. \tag{45}$$

If we approximate

$$\frac{\mathrm{d}R(t)}{\mathrm{d}t}\bigg|_{t=t_{j+1}} \approx \frac{r_{j+1}-r_j}{\tau} = \frac{h_{j+1}}{\tau}, \tag{46}$$

then the boundary condition (40) can be discretized in the form

$$\frac{h_{j+1}}{\tau} + d(\phi_j^{j-1},\phi_j^j)\frac{\phi_{j+1}^{j+1}-\phi_j^{j+1}}{h_{j+1}} - \frac{q_{\ell\mathrm{m,in}}R_{\mathrm{out}}}{r_j} = 0, \tag{47}$$

where we define

$$d(\phi_{j-1}^j,\phi_j^j) := \frac{\varepsilon_s^0}{\varepsilon_s^0-\varepsilon_{s0}}\frac{k^0}{2\mu}\Big((\eta_{s,j}^j)^{-\delta} + (\eta_{s,j-1}^j)^{\delta}\Big). \tag{48}$$

The initial condition (31) is discretized by setting

$$\phi_i^0 = 0, \quad i = 0,1,\dots, \tag{49}$$

the boundary condition (32) is implemented by

$$\phi_i^{j+1} = 0, \quad i = j+2, j+3,\dots, \quad j = 0,1,2\dots, \tag{50}$$

and the boundary condition (41) is discretized by

$$-g(\phi_0^j)\frac{\phi_1^j-\phi_0^j}{h_1} = \frac{q_{\ell\mathrm{m,in}}R_{\mathrm{out}}}{r_{\mathrm{m}}}, \quad j = 0,1,\dots. \tag{51}$$

Notice that the numerical solution at time t_{j+1} consists of $j+3$ unknowns, namely ϕ_i^{j+1} for $i = 0,\dots,j+1$ plus h_{j+1}, for which the same number of scalar equations is available, namely the j equations (43), the boundary condition (50), the boundary condition (51), and (47).

3.2 *Solution of the nonlinear system*

The resulting system of equations (43) and (47), complemented by initial and boundary conditions, is nonlinear. We solve it approximately by the simple iteration method

$$-g(\phi_0^{(\lambda),j})\frac{\phi_1^{(\lambda+1),j}-\phi_0^{(\lambda+1),j}}{h_1} = \frac{q_{\ell\mathrm{m,in}}R_{\mathrm{out}}}{r_{\mathrm{m}}}, \tag{52}$$

$$\begin{aligned}&\frac{\phi_i^{(\lambda+1),j+1}-\phi_i^j}{\tau} - \frac{2a(\phi_i^{(\lambda),j+1})}{r_i(h_i+h_{i+1})}\times\\ &\times\Delta_-\Big(b(\phi_i^{(\lambda),j+1},\phi_{i+1}^{(\lambda),j+1})r_{i+1/2}\frac{\phi_{i+1}^{(\lambda+1),j+1}-\phi_i^{(\lambda+1),j+1}}{h_{i+1}}\Big)\\ &+\frac{q_{\ell\mathrm{m,in}}R_{\mathrm{out}}}{r_{i-1/2}}\frac{\phi_i^{(\lambda+1),j+1}-\phi_{i-1}^{(\lambda+1),j+1}}{h_i} = 0, \quad i = 1,\dots,j,\end{aligned} \tag{53}$$

$$\begin{aligned}&-\frac{h_{j+1}^2}{\tau} + \frac{q_{\ell\mathrm{m,in}}R_{\mathrm{out}}}{r_j}h_{j+1} - d(\phi_j^{(\lambda),j+1},\phi_{j+1}^{(\lambda),j+1})\times\\ &\times(\phi_{j+1}^{(\lambda+1),j+1}-\phi_j^{(\lambda+1),j+1}) = 0,\end{aligned} \tag{54}$$

where λ is an iteration number and $b(\phi_i^{(\lambda),j+1},\phi_{i+1}^{(\lambda),j+1})$ is defined analogously to (44). Notice that (52)–(54) is a system of $j+2$ equations that is *linear* in $\phi_i^{(\lambda+1),j+1}$, $i = 0,\dots,j+1$, which allows the use of the sweep method. The solution of (52)–(54) requires that we specify h_{j+1}. To this end we define an initial guess $h_{j+1} := h_{j+1}^{\mathrm{init}}$, for instance $h_{j+1}^{\mathrm{init}} := h_j$, which is corrected once the solution for ϕ_i^{j+1} is determined. Consequently, for given ϕ_i^j, $i = 0,\dots,j+1$, we compute ϕ_i^{j+1} for $i = 0,\dots,j+1$ as follows.

1. Set $\lambda := 0$, $\phi_i^{(0),j+1} := \phi_i^j$ for $i = 0,\dots,j+1$, and $h_{j+1} := h_{j+1}^{\mathrm{init}} := h_j$.
2. To compute $y_i := \phi_i^{(\lambda+1),j+1}$ for $i = 0,\dots,j+1$ we solve the linear system (52)–(54) This system is of tridiagonal form and it can be easily be solved by the Thomas algorithm (see the appendix).
3. Assume that $\Delta > 0$ is a given accuracy, and let
$$\mathcal{E} := \max_{0\le i\le j+1}\Big|\phi_i^{(\lambda+1),j+1} - \phi_i^{(\lambda),j+1}\Big|. \tag{55}$$
If $\mathcal{E} \le \Delta$, then we set $\phi_i^{j+1} := \phi_i^{(\lambda),j+1}$. Otherwise, we increase λ by one and continue with (2).
4. Once ϕ_i^{j+1} is determined for $i = 0,\dots,j+1$, we utilize (54) to determine the final value of h_{j+1}. This equation can be written as
$$\begin{aligned}&\frac{h_{j+1}^2}{\tau} - \frac{q_{\ell\mathrm{m,in}}R_{\mathrm{out}}}{r_j}h_{j+1}\\ &+d(\phi_j^{j+1},\phi_{j+1}^{j+1})(\phi_{j+1}^{j+1}-\phi_j^{j+1}) = 0.\end{aligned} \tag{56}$$
Solving this quadratic equation at each time layer we determine h_{j+1}. (Among the two roots of the quadratic equation, the positive root that has physical meaning is selected.)

4 Numerical results

Numerical results of the procedure outlined in Section *3.2* were obtained for the values of the initial parameters $q_{\ell\mathrm{m,in}}R_{\mathrm{out}} = 2\cdot10^{-5}\,\mathrm{m}^2/\mathrm{s}$, $p_A = 10^3\,\mathrm{Pa}$, $\mu = 10^{-3}\,\mathrm{Pa\,s}$, $k^0 = 3.4965\cdot10^{-13}\,\mathrm{m}^2$, $\varepsilon_s^0 = 0.269$, $\varepsilon_{s0} = 0.2$, $\beta = 0.09$, and $\delta = 0.49$.

Some results are shown in Figures 4 to 8. As can be seen from the presented results, as the filtration process continues, the cake layer thickness increases (Figure 4), and a compression pressure distribution is established throughout its thickness. Figure 5(a) shows the compressive pressure profiles for several fixed time values. According to the

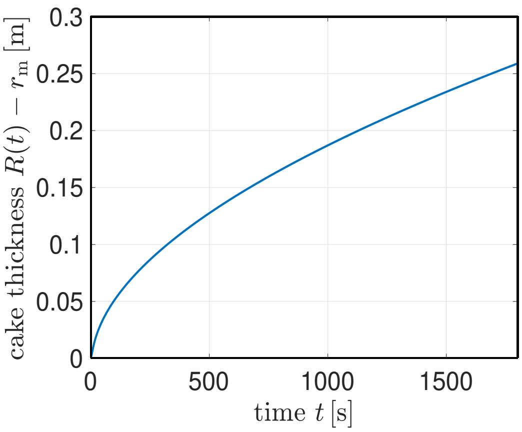

Fig. 5. Dynamics of sediment layer thickness on the filter surface.

assumptions adopted in this model, the compressive pressure decreases from the filter surface toward the cake layer/suspension boundary. Over time, the compressive pressure increases at all points along the cake layer. The compressive pressure distribution precisely terminates at zero at the cake layer/suspension boundary. Figure 5(b) shows graphs of the solids content ε_s for several fixed points in time. It is clear from (11) that ε_s varies according to a power-law dependence on p_s. Therefore, the compression pressure profiles shown in Figure 5(a) decrease in the direction from $r = r_m$ to $R = R(t)$. As the cake layer thickness increases, the profiles of the distribution of ε_s increase over time. Due to the compaction of the cake layer, the solids content is higher on the filter surface. In contrast to ε_s, the relative permeability k/k^0 increases from the filter surface toward the cake layer/slurry boundary (Figure 5(c)). Over time, relative permeability decreases at all points in the cake layer. This indicates an increase in filtration resistance. The dynamics of concentration and relative permeability at a given point in the sediment are determined similarly (Figure 6). The graphs show a lagging dynamics of porosity and an advancing dynamics of relative permeability of the sediment. Some numerical results with increased values of β are shown in Figure 7. Increasing this parameter in accordance with (11) can lead to higher solids content values. An increase in the number of solid particles is observed on the filter surface. Calculations of filtration characteristics were performed for various values of δ. Some results are presented in Figure 8. As can be seen from the graphs, increasing the value of δ leads to an increase in pressure p_s distribution and solid content ε_s in the cake layer, while relative permeability decreases.

5 Conclusions

This article considers the process of filtering a suspension through a cylindrical filter at a constant flow rate. As the suspension passes through the filter, suspended particles are retained and form a sediment layer on the filter surface. Local cake layer properties, such as solids content and permeability, were represented as functions of compressive pressure, using power functions to describe them. Taking these relationships into account, filtration equations for compressive pressure were derived from the cake layer filtration equation. Compressive pressure distributions across the cake layer and cake layer thickness growth were determined. Over time, compressive pressure increases at all points of the cake layer. Over time, compressive pressure decreases from the filter surface to the cake layer/suspension interface. This indicates that suspended particles are compacted on the filter surface. The compression pressure profile distribution expands, remaining zero at the cake layer/suspension boundary. Over time, the cake layer thickness increases monotonically at the filter surface, and the solids concentration at this surface is higher than the concentration in the rest of the cake layer. This pattern of solids concentration variation determines the solids content distribution within the cake layer, with the solids content decreasing in the direction from $r = r_m$ to $R(t)$.

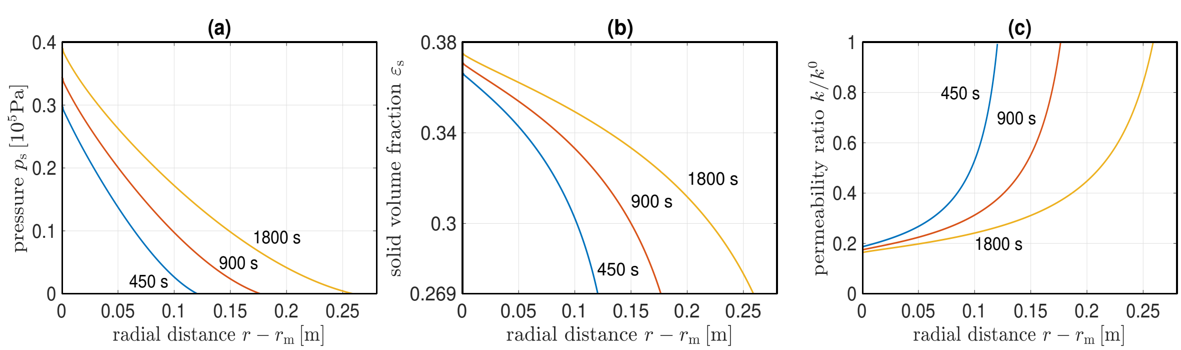

Fig. 6. Distribution of (a) p_s, (b) ε_s and (c) k/k^0 at simulated times $t = 450\,$s, $t = 450\,$s, and $t = 1800\,$s.

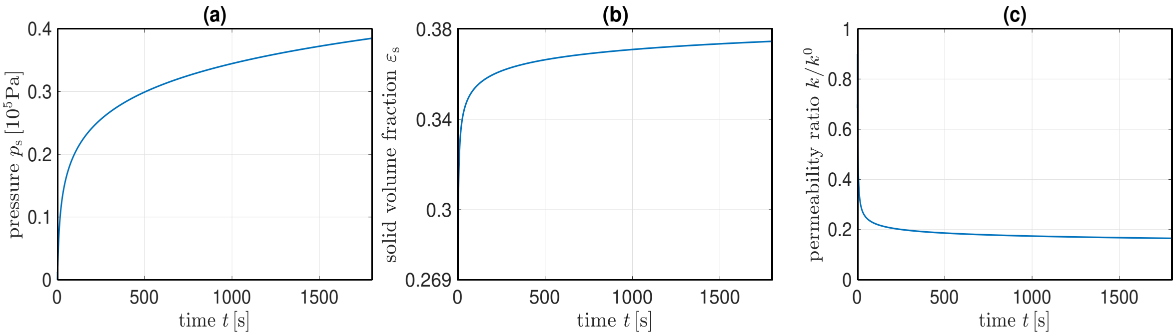

Fig. 7. Dynamics of (a) p_s, (b) ε_s and (c) k/k^0 at fixed radial position $r - r_m = 0.002\,$m.

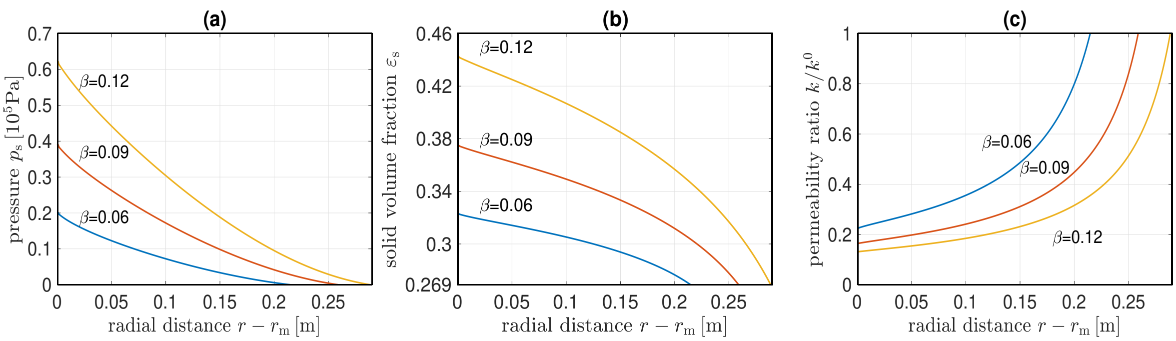

Fig. 8. Profiles of (a) p_s, (b) ε_s and (c) k/k^0 at simulated time $t = 1800\,$s with the parameter values $\beta = 0.06$, $\beta = 0.09$, and $\beta = 0.12$.

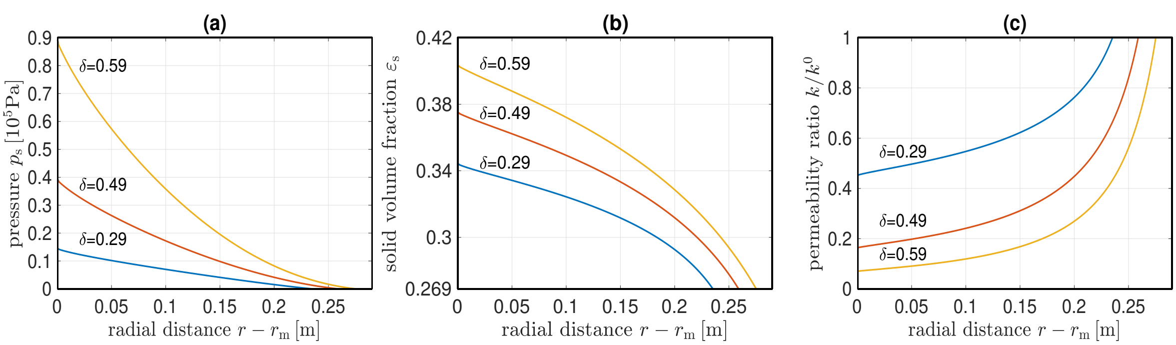

Fig. 9. Profiles of (a) p_s, (b) ε_s and (c) k/k^0 at simulated time $t = 1800\,$s with the parameter values $\delta = 0.29$, $\delta = 0.49$, and $\delta = 0.59$.

The influence of the parameters δ and β, which are included in the dependence of permeability and solids concentration on compression pressure, on filtration performance was assessed. It was shown that increasing the value of δ leads to a decrease in cake layer permeability, which in turn increases the compression pressure and solids concentration. Increasing the value of β has a similar effect. As the filtration rate of the suspension increases, cake layer consolidation increases, leading to an increase in compression pressure and particle concentration on the filter, as well as a decrease in permeability. Thus, the numerical solution of the model developed in this work for the filtration of a suspension through a cylindrical filter at constant flow rate was found to be consistent with physical expectations regarding cake compaction and pressure buildup, and close agreement was obtained between the numerical results and the explicit analytical solution available for the incompressible-cake limiting case, which supports the accuracy and physical consistency of the proposed free-boundary formulation for the compressible-cake case considered here.

In this study, the focus is placed on the constitutive parameters of the model (k^0, ε_s^0, β, and δ) rather than individual operational variables such as inlet concentration and particle size distribution (PSD); that is, the proposed model is based on a standard macroscopic continuum approach (Tien, 2006), where the physical effects of the inlet suspension characteristics are implicitly accounted for within the empirically determined constitutive parameters.

The present model simultaneously combines three features: cylindrical radial geometry, constant rate filtration conditions, and a compressible cake governed by power-law constitutive relations within a fully coupled free-boundary formulation. This combination yields a physically more consistent description of cake growth and compressive pressure evolution under CRF conditions than is attainable with existing planar or constant-pressure models, and the close agreement obtained between the numerical solution and the explicit analytical solution available for the incompressible-cake limiting case confirms the validity of the proposed extended formulation.

In contrast to the works by Kalantariasl et al. cited in Section 1, the present paper addresses the filtration of a suspension through an industrial cylindrical filter; adopts constant rate filtration (CRF) conditions, which, unlike constant pressure filtration, allow the filter medium resistance R_{m} to be determined accurately from the intercept of the pressure–time curve; accounts for cake compressibility and permeability as power-law functions of the compressive pressure p_{s}; and takes p_{s} as the primary unknown, formulating a single, unified numerical solution system coupled with the evolution equation for the moving boundary $R(t)$. The analytical formulae proposed by Kalantariasl et al. (2014) for the incompressible-cake case provide a natural benchmark for validating the numerical solution of the present model in the limiting case $\beta \to 0$, $\delta \to 0$, in which the compressible-cake formulation degenerates to the incompressible one. When β and δ are non-zero, however, the governing system of equations derived in the present work does not admit a closed-form analytical solution, and numerical solution of the full system is the only viable approach to obtaining an accurate approximation to the solution in the general compressible-cake case.

With respect to future directions of research, we recall that the prime contribution of this work has been the development and analysis of a mathematical model for radial filtration specifically under CRF conditions. That said, and aiming at industrial applications, we mention that in the oil and gas industry, radial flow through cylindrical filter cartridges and well-completion screens arises during drilling fluid filtration (cf., e.g., Rodríguez-López et al., 2025) and during the injection of particle-laden fluids into wellbores, where constant rate operation is standard practice; accurate prediction of cake buildup and the resulting injectivity decline can be directly applied to well-completion design.

Another direction of future research concerns the assumption that the filter medium resistance R_{m} is kept constant. In fact, the present model is restricted to the case in which solid particles are retained on the outer surface of the filter and form a compressible cake; pore plugging filtration, in which particles penetrate and become trapped within the pores of the filter medium, was beyond the scope of this work and may be addressed in future investigations.

We also mention that the constitutive parameters used in this work (k^0, $\varepsilon_{\mathrm{s}}^0$, β, δ, and p_A) are in principle measurable from standard compression-permeability cell experiments for a given suspension, and the total pressure drop $\Delta p(t)$ predicted by the model is in principle directly comparable with experimental pressure–time measurements under CRF conditions of the type reported by Mahdi and Holdich (2013, 2017) and Mahdi et al. (2019). A direct experimental validation of the radial CRF model developed here would require a purpose-built cylindrical filtration cell operated at constant flow rate, with measurements of the pressure drop across the system as a function of time and, if possible, cake thickness measurements via, e.g., ultrasonic or X-ray tomographic techniques. Such an experimental campaign is beyond the scope of the present theoretical work but is identified as an essential and high-priority direction for future research.

The present approach has been based on using the solid pressure p_{s} within the cake as main unknown. Future research will focus on the transition to using the solids volume fraction ε_{s} as the primary unknown within a CRF framework, as was done e.g. in Bürger et al. (2001). This transition should allow for a unified treatment of the solids volume fraction both in the filter cake as well as the surrounding suspension.

Acknowledgements

R.B. is supported by ANID (Chile) through Fondecyt project 1250676; Centro de Modelamiento Matemático (CMM), BASAL project FB210005; and project AMSUD250028 "Structured meta-populations in epidemiology and ecology: modeling and control (StrucMetaMoC)."

Appendix: The Thomas algorithm

The linear system of $j+2$ scalar equations defined by (53) and the boundary condition (51) can be written as

$$\begin{aligned} C_0 y_0 - B_0 y_1 &= F_0, \\ -A_i y_{i-1} + C_i y_i - B_i y_{i+1} &= F_i, \quad i = 1,\dots,j, \\ -A_{j+1} y_j + C_{j+1} y_{j+1} &= F_{j+1}, \end{aligned} \tag{A.1}$$

where we define $C_0 := 1$, $B_0 := 1$,

$$\begin{aligned} F_0 &:= \frac{h_1}{g(\phi_0^{(\lambda),j})} \cdot \frac{q_{\ell\mathrm{m,in}} R_{\mathrm{out}}}{r_{\mathrm{m}}}, \\ A_i &:= \frac{2a(\phi_i^{(\lambda),j+1}) b(\phi_{i-1}^{(\lambda),j+1}, \phi_i^{(\lambda),j+1}) r_{i-1/2}}{r_i(h_i + h_{i+1}) h_i} \\ &\quad + \frac{q_{\ell\mathrm{m,in}} R_{\mathrm{out}}}{r_{i-1/2} h_i}, \quad i = 1,\dots,j, \\ C_i &:= \frac{1}{\tau} + \frac{2a(\phi_i^{(\lambda),j+1})}{r_i(h_i + h_{i+1})} \biggl(\frac{b(\phi_i^{(\lambda),j+1}, \phi_{i+1}^{(\lambda),j+1})}{h_{i+1}} r_{i+1/2} \\ &\quad + \frac{b(\phi_{i-1}^{(\lambda),j+1}, \phi_i^{(\lambda),j+1})}{h_i} r_{i-1/2} \biggr) + \frac{q_{\ell\mathrm{m,in}} R_{\mathrm{out}}}{r_{i-1/2} h_i}, \\ &\quad i = 1,\dots,j, \\ B_i &:= \frac{2a(\phi_i^{(\lambda),j+1}) b(\phi_i^{(\lambda),j+1}, \phi_{i+1}^{(\lambda),j+1}) r_{i+1/2}}{r_i(h_i + h_{i+1}) h_{i+1}}, \\ &\quad i = 1,\dots,j, \\ F_i &:= \phi_i^j / \tau, \quad i = 1,\dots,j, \\ A_{j+1} &:= -d(\phi_j^{(\lambda),j+1}, \phi_{j+1}^{(\lambda),j+1}), \quad C_{j+1} = A_{j+1}, \\ F_{j+1} &:= \frac{h_{j+1}^2}{\tau} - \frac{q_{\ell\mathrm{m,in}} R_{\mathrm{out}}}{r_j} h_{j+1}, \end{aligned} \tag{A.2}$$

and it is understood that $h_{j+1} = h_{j+1}^{\mathrm{init}}$.

The Thomas algorithm can be employed to solve (A.1) as follows. We seek a solution of in the form

$$y_{j+1} = \zeta_{j+1}; \quad y_i = \xi_i y_{i+1} + \zeta_i, \quad i = j, j-1, \dots, 1, 0. \tag{A.3}$$

The coefficients ζ_i and ξ_i are computed by first computing successively

$$\xi_i = \begin{cases} -B_0/C_0 & \text{for } i = 0, \\ -B_i/(C_i + A\xi_{i-1}) & \text{for } i = 1,2,\dots,j-1,j \end{cases} \tag{A.4}$$

and then

$$\zeta_i = \begin{cases} F_0/C_0 & \text{for } i = 0, \\ (F_i + A_i \zeta_{i-1})/(C_i + A_i \xi_i) & \text{for } i = 1,2,\dots,j,j+1. \end{cases} \tag{A.5}$$

Notice that the starting values of the coefficients, ξ_0 and ζ_0, are determined from the boundary condition (52), hence we can compute all required coefficients ξ_i and ζ_i.

Nomenclature

$a(\cdot)$	auxiliary function defined in Eq. (38)
$b(\cdot)$	auxiliary function defined in Eq. (38)
$b(\cdot,\cdot)$	auxiliary function defined in Eq. (44)
$d(\cdot)$	auxiliary function defined in Eq. (38)
$d(\cdot,\cdot)$	auxiliary function defined in Eq. (48)
$\mathcal{E}$	convergence test quantity defined in Eq. (55)
$\mathcal{F}(\cdot)$	filtration rate function defined in Eq. (4)
$g(\cdot)$	auxiliary function defined in Eq. (38)
h	height of the cylindrical filter [m]
h_j	difference $h_j = r_j - r_{j-1}$ (see Figure 3) [m]
h_j^{init}	initial guess for h_{j+1} [m]
k	permeability of the cake layer [m^2]
k^0	permeability of cake layer at zero compressive stress [m^2]
p_A	characteristic pressure in Eq. (11) [Pa]
p_ℓ	pressure in liquid phase [Pa]
p_{s}	compressive pressure [Pa]
q_ℓ	filtration rate of liquid phase [m/s]
$q_{\ell\mathrm{i}}$	filtration rate for cake layer [m/s]
$q_{\ell\mathrm{o}}$	filtration rate for suspension zone [m/s]
$q_{\ell\mathrm{m}}$	total filtration rate [m/s]
$q_{\ell\mathrm{m,in}}$	total filtration rate at $r = R_{\mathrm{out}}$, Eq. (30) [m/s]
q_{s}	filtration rate of solid phase [m/s]
r	radial coordinate [m]
r_i	node of spatial grid [m]
r_{m}	outer radius of filter medium [m]
R_{m}	hydraulic resistance of filter medium [m^{-1}]
$R(t)$	cake layer thickness [m]
t	time [s]
t_j	time point in numerical simulation [s]
R	time-dependent cake-suspension interface [m]
v_ℓ, $\boldsymbol{v}_\ell$	liquid phase velocity [m/s]
v_{s}, $\boldsymbol{v}_{\mathrm{s}}$	solid phase velocity [m/s]
V_{acc}	control volume related to moving boundary defined in Eq. (19) [m^3]
V_{in}	control volume related to moving boundary defined in Eq. (17) [m^3]
V_{out}	control volume related to moving boundary defined in Eq. (18) [m^3]
β	dimensionless exponent in Eq. (11)
δ	dimensionless exponent in Eq. (11)
ε	dimensionless porosity of cake layer
ε_{s}	dimensionless solid volume fraction (solidosity) of cake layer
$\varepsilon_{\mathrm{s0}}$	dimensionless solid volume fraction of particles in suspension
$\varepsilon_{\mathrm{s}}^0$	dimensionless solid content at zero stress
η_{s}	auxiliary quantity defined in Eq. (34)
$\eta_{\mathrm{s}i}^j$	auxiliary quantity defined in Eq. (42)
λ	dimensionless iteration number
μ	viscosity of suspension [Pa s]
ϕ_i^j	approximate value of p_{s} at (t_j, r_i) [Pa]
τ	time step for numerical simulation [s]

References

Almy, C. and Lewis, W. K. (1912). Factors determining the capacity of a filter press. *J. Indust. Eng. Chem.*, 4:528–532. https://doi.org/10.1021/ie50043a026

Atsumi, K. and Akiyama, T. (1975). A study of cake filtration—formulation as a Stefan problem. *J. Chem. Engrg. Japan*, 8(6):487–492. https://doi.org/10.1252/jcej.8.487

Bastida-Vázquez, J. J., Roa-Morales, G., Gómez-Espinosa, R. M., Balderas-Hernández, P. and Natividad-Rangel, R. (2024). Water treatment applying electrocoagulation and filtration processes with a functionalized membrane of a contaminated water body from San Cayetano de Morelos, Toluca. *Rev. Mex. Ing. Quím.*, 23(1):IA24164. https://rmiq.org/iqfvp/Numbers/V23/No1/IA24164.pdf

Bürger, R., Concha, F., and Karlsen, K. H. (2001). Phenomenological model of filtration processes: 1. Cake formation and expression. *Chem. Eng. Sci.*, 56(15):4537–4553. https://doi.org/10.1016/S0009-2509(01)00115-4

Bürger, R., Frid, H., and Karlsen, K. H. (2003). On a free boundary problem for a strongly degenerate quasi-linear parabolic equation with an application to a model of pressure filtration. *SIAM J. Math. Anal.*, 34(3):611–635. https://doi.org/10.1137/S0036141002401007

Caldwell, J. and Kwan, Y. Y. (2004). Numerical methods for one-dimensional Stefan problems. *Comm. Numer. Methods Engrg.*, 20(7):535–545. https://doi.org/10.1002/cnm.691

Concha A., F. and Bascur, O. A. (2024). *The Engineering Science of Mineral Processing*. CRC Press, Boca Raton, FL, USA. 525pp.

Escobar, B., Baas-López, J. M., Tapia-Tussell, R. and Olguín-Maciel, E. (2024). Biochar-packed biofilter for the treatment of gases produced by accumulated *Sargassum* waste. *Rev. Mex. Ing. Quím.*, 23(2):Bio24219. https://rmiq.org/iqfvp/Numbers/V23/No2/Bio24219.pdf

Garrido, P., Concha, F., and Bürger, R. (2003). Settling velocities of particulate systems: 14. Unified model of sedimentation, centrifugation and filtration of flocculated suspensions. *Int. J. Mineral Process.*, 72:57–74. https://doi.org/10.1016/S0301-7516(03)00087-5

Greil, P., Gruber, U., Travitzky, N., and Kulig, M. (1992). Pressure filtration of silicon nitride suspensions with constant filtration rate. *Mater. Sci. Engrg.*, A151:247–254. https://doi.org/10.1016/0921-5093(92)90213-K

Iritani, E. (2003). Properties of filter cake in cake filtration and membrane filtration. *KONA*, 21:19–39. https://doi.org/10.14356/kona.2003007

Iritani, E., Katagiri, N., and Youshida, T. (2018). Simplified evaluation of consolidation and expansion behaviour of highly compressible cake. *Filtration*, 18(1):50–60.

Kalantariasl, A., and Bedrikovetsky, P. (2014). Stabilization of external filter cake by colloidal forces in a "well-reservoir" system. *Ind. Engrg. Chem. Res.*, 53:930–944. https://doi.org/10.1021/ie402812y

Kalantariasl, A., Zeinijahromi, A., and Bedrikovetsky, P. (2014). Axi-symmetric two-phase suspension-colloidal flow in porous media during water injection. *Ind. Engrg. Chem. Res.*, 53:15763–15775. https://doi.org/10.1021/ie502312c

Kalantariasl, A., Farajzadeh, R., You, Z., and Bedrikovetsky, P. (2015). Nonuniform external filter cake in long injection wells. *Ind. Engrg. Chem. Res.*, 54:3051–3061. https://doi.org/10.1021/ie504936q

Khuzhayorov, B. K., Ibragimov, G., Saydullaev, U., and Pansera, B. A. (2023). An axi-symmetric problem of suspensions filtering with the formation of a cake layer. *Symmetry*, 15(6):1209. https://doi.org/10.3390/sym15061209

Khuzhayorov, B. K., Ibragimov, G., Saydullaev, U., Shadmanov, I., and Ali, F. M. (2022a). Filtration of suspensions with forming of an elastoplastic cake. *Waves Random Complex Media*, 32:1–24. https://doi.org/10.1080/17455030.2022.2136417

Khuzhayorov, B. K., Saydullaev, U., Ibragimov, G., and Wahi, N. (2022b). An axisymmetric problem of suspension filtering with formation of elastic-plastic cake layer. *Symmetry*, 14(6):1202. https://doi.org/10.3390/sym14061202

King, C. J. (1980). *Separation Processes*. McGraw-Hill, New York, second edition. 850pp.

Mahdi, F. M. and Holdich, R. G. (2013). Laboratory cake filtration testing using constant rate. *Chem.

Eng. Res. Des., 91(6):1145–1154. https://doi.org/10.1016/j.cherd.2012.11.012

Mahdi, F. M. and Holdich, R. G. (2017). Using statistical and artificial neural networks to predict the permeability of loosely packed granular materials. *Sep. Sci. Technol.*, 52:1–12. https://doi.org/10.1080/01496395.2016.1232735

Mahdi, F. M., Hunter, T. N., and Holdich, R. G. (2019). A study of cake filtration parameters using the constant rate process. *Processes*, 7:746. https://www.mdpi.com/2227-9717/7/10/746

Rodríguez-López, L. C., Pérez-Vidal, H., Gómez-Torres, F. C., Martínez-Pacheco, C., Uicab-Córdova, E. E., Madrigal-Díaz, S. C. and Díaz-Flores, L. L. (2025) Enhancement of rheological and filtration properties of water-based drilling fluids through zinc oxide nanoparticles addition. *Rev. Mex. Ing. Quím.*, 24(2):IA25505. https://rmiq.org/iqfvp/Numbers/V24/No2/IA25505.pdf

Ruth, B. F. (1935). Derivation of general filtration equations. *Ind. Engrg. Chem.*, 27:708–723. https://doi.org/10.1021/ie50306a024

Samarsky, A. A. and Vabishchevich, P. N. (2003). *Computational Heat Transfer*. M.: Editorial URSS. 784pp. In Russian.

Shirato, M., Murase, T., Iwata, M., and Nakatsuka, S. (1986). The Terzaghi-Voigt combined model for constant-pressure consolidation of filter cakes and homogeneous semi-solid materials. *Chem. Eng. Sci.*, 41(12):3213–3218. https://doi.org/10.1016/0009-2509(86)85059-X

Shirato, M., Sambuichi, M., Kato, H., and Aragaki, T. (1969). Internal flow mechanism in filter cakes. *AIChE J.*, 15(3):405–409. https://doi.org/10.1002/aic.690150320

Smiles, D. E. (1970). A theory of constant pressure filtration. *Waves Random Complex Media*, 25:985–996. https://doi.org/10.1016/0009-2509(70)85043-6

Sparks, T. and Chase, G. (2015). *Filters and Filtration Handbook*. Butterworth-Heinemann, Woburn, MA, USA, sixth edition. 440 pp.

Stamatakis, K. and Tien, C. (1991). Cake formation and growth in cake filtration. *Chem. Eng. Sci.*, 46:1917–1933. https://doi.org/10.1016/0009-2509(91)80153-P

Stauffer, P. H. (2006). Flux flummoxed: A proposal for consistent usage. *Ground Water*, 44(2):125–128. https://doi.org/10.1111/j.1745-6584.2006.00197.x

Tarabara, V. V., Hovinga, R. M., and Wiesner, M. R. (2002). Constant transmembrane pressure vs. constant permeate flux: effect of particle size on crossflow membrane filtration. *Environ. Eng. Sci.*, 19(6):343–355. https://doi.org/10.1089/109287502320963355

Tien, C. (2006). *Introduction to Cake Filtration: Analysis, Experiments, and Applications*. Elsevier, Amsterdam. 304 pp.

Tien, C. (2012). *Principles of Filtration*. Elsevier.

Tien, C. and Bai, R. (2003). An assessment of the conventional cake filtration theory. *Chem. Eng. Sci.*, 58(7):1323–1336. https://doi.org/10.1016/S0009-2509(02)00655-3

Tien, C. and Ramarao, B. V. (2007). *Granular Filtration of Aerosols and Hydrosols*. Elsevier, Amsterdam. 512 pp.

Tien, C., Teoh, S. K., and Tan, R. B. H. (2001). Cake filtration analysis—the effect of the relationship between the pore liquid pressure and the cake compressive stress. *Chem. Eng. Sci.*, 56:5361–5369. https://doi.org/10.1016/S0009-2509(01)00263-9

Tiller, F. M. (1953). The role of porosity in filtration I — Numerical methods for constant rate and constant pressure filtration based on Kozeny's law. *Chem. Eng. Progr.*, 49(9):467–479.

Tiller, F. M. and Leu, W. F. (1980). Basic data fitting in filtration. *J. Chinese Inst. Chem. Engrs.*, 11:61–70.

Tosun, I. (1986). Formulation of cake filtration. *Chem. Eng. Sci.*, 41(10):2563–2568. https://doi.org/10.1016/0009-2509(86)80042-2

Vorobiev, E. (2022). Dewatering of non-uniformly structured wet compacts under additional compressive pressure: Predictive model. *Powder Technol.*, 404:117469. https://doi.org/10.1016/j.powtec.2022.117469

Wakeman, R. J. (1978). A numerical integration of the differential equations describing the formation of and flow in compressible filter cakes. *Trans. Inst. Chem. Eng.*, 56(4):258–265.

Wakeman, R. J. and Tarleton, E. S. (1999). *Filtration. Equipment Selection Modelling and Process Simulation*. Elsevier Advanced Technology, New York. 446 pp.

Yim, S. S., Song, Y. M., and Kwon, Y. D. (2003). The role of p_i, p_o, and p_f in constitutive equations and new boundary conditions in cake filtration. *Korean J. Chem. Eng.*, 20(2):334–342. https://doi.org/10.1007/BF02697249

Zhuzhikov, V. A. (1980). *Theory and Practice of Separation of Suspensions*. Khimiia Publishing, Moscow, Russia. 440 pp.